Aquat Geochem (2007) 13:157–172
DOI 10.1007/s10498-007-9013-0

REVIEW

Transient States in Diagenesis Following the Deposition of a Gravity Layer: Dynamics of O_2, Mn, Fe and N-Species in Experimental Units

Gwénaëlle Chaillou · Pierre Anschutz · Carole Dubrulle · Pascal Lecroart

Received: 9 October 2006 / Accepted: 22 May 2007 / Published online: 4 July 2007

Abstract Biogeochemical processes induced by the deposition of gravity layer in marine sediment were studied in a 295-day experiment. Combining voltammetric microelectrode measurements and conventional analytical techniques, the concentrations of C, O_2, N-species, Mn and Fe have been determined in porewaters and sediments of experimental units. Dynamics of the major diagenetic species following the sudden sediment deposition of few cm-thick layer was explained by alternative diagenetic pathways whose relative importance in marine sediments is still a matter of debate. Time-series results indicated that the diffusion of O_2 from overlying waters to sediments was efficient after the deposition event: anoxic conditions prevailed during the sedimentation. After a few days, a permanent oxic horizon was formed in the top few millimetres. At the same time, the oxidation of Mn^{2+} and then Fe^{2+}, which diffused from anoxic sediments, contributed to the surficial enrichment of fresh Mn(III/IV)- and Fe(III)-oxides. Vertical diffusive fluxes and mass balance calculations indicated that a steady-state model described the dynamic of Mn despite the transitory nature of the system. This model was not adequate to describe Fe dynamics because of the multiple sources and phases of Fe^{2+}. No significant transfer of Mn and Fe was observed between the underlying sediment and the new deposit: Mn- and Fe-oxides buried at the original interface acted as an oxidative barrier to reduced species that diffused from below. Nitrification processes led to the formation of a NO_3^-/NO_2^- rich horizon at the new oxic horizon. Over the experiment period, NO_3^- concentrations were also measured in the anoxic sediment suggesting anaerobic nitrate production.

G. Chaillou (✉) · P. Anschutz · C. Dubrulle · P. Lecroart
Environnements et Paléoenvironnements OCeaniques (EPOC), UMR CNRS 5805, Université Bordeaux 1, 33405 Talence, France
e-mail: gwenaelle_chaillou@uqar.qc.ca

P. Anschutz
e-mail: p.anschutz@epoc.u-bordeaux1.fr

P. Lecroart
e-mail: p.lecroart@epoc.u-bordeaux1.fr

Present Address:
G. Chaillou
ISMER/UQAR, 310 Allée des Ursulines, Rimouski, QC, Canada G5L 3A1

Keywords Diagenesis · Alternative biogeochemical pathways · Gravity deposit · Laboratory experiment · Microelectrodes · Sedimentary biogeochemistry

1 Introduction

Although early diagenesis in marine sediments is often described as a steady-state phenomenon (Berner 1980; Froelich et al. 1979), the geochemical composition of sediments evolves via transient states because of changes in organic carbon input, oxygen content of bottom water, sedimentation rate or biological activity (Sundby 2006). Seabed reworking caused by sediment-resuspension, -transport and -deposition as well as low-frequency disturbances such as large storms and mass flows has also a tremendous impact on diagenetic reactions and the hosted benthic community (Aller 1989; Anschutz et al. 2002; Deflandre et al. 2002; Saulnier and Mucci 2000).

The microbial-mediated oxidation of organic matter based on the use of the electron acceptor that yields to the highest amount of free energy in the terminal electron transfer step is usually considered to explain the depth distribution of metabolites in sediments ($O_2 > NO_3^-$–Mn-oxides > Fe-oxides > $SO_4^{2-} > CO_2$; Froelich et al. 1979). The contribution of these various metabolic pathways to carbon degradation varies temporally and spatially due to changes in acceptor (and donors) abundance. Numerous alternative biochemical pathways that include oxidant regeneration by oxygen as well as anaerobic mechanisms are also thermodynamically favourable at pH values encountered in marine sediments. The contribution of these processes that proceed by both abiotic and biotic pathways to the overall carbon degradation is largely unknown although they might be quantitatively important (Megonigal et al. 2004 and references therein). Seabed reworking of marine sediments, particularly gravity deposits, yields either the remobilization or the immobilization of chemical substances, which have unique responses to the redox gradient developed in the new material and in the underlying sediment (Anschutz et al. 2002; Deflandre et al. 2002; Mucci and Edenborn 1992; Mucci et al. 2003). Alternative biochemical pathways which become perceptible under these non-steady state conditions, could mainly contribute to the spatial distribution of metabolites over prolonged periods (i.e. months to years). Investigations of redox-sensitive trace metals on distal turbidites reveal that disruptions of the ongoing diagenesis persist also over geological periods (Buckley and Cranston 1988; Colley and Thomson 1985; De Lange 1986; Jarvis et al. 1988) because paleo-oxidation zones developed over periods of a few thousands to several hundreds of thousands years have been imprinted in the sedimentary column.

Although there are several studies on the evolution of sediment and porewater chemistry in recent turbidites (Anschutz et al. 2002; Deflandre et al. 2002; Mucci et al. 2003; Mucci and Edenborn 1992), there is little information on the first diagenetic steps following sudden episodic deposition of new material on the seabed. Since field observations of ongoing gravity deposit are complex, we present in this study the results of a 295-day experiment that simulated the biogeochemical processes that occur days and weeks that follow the deposition of a gravity layer. Our experimental set-up was not intended to reproduce the complex energetic system of surge flow and, consequently, cannot be related directly to natural environmental conditions. However, our experimental results add new information to non-steady state diagenetic reactions following a sedimentary perturbation, which is valid in natural conditions. Experiments were prepared to create a grain-size fining-up sequence by gravity deposition, as observed in turbidite deposits. By combining conventional analytical

techniques and voltammetric microelectrodes, we monitored the vertical distribution and the concentrations of C_{org}, dissolved O_2, N-species (NO_3^-, NO_2^- and NH_4^+) with emphasis on Mn and Fe cycles because of their pivotal role on diagenetic behaviour of many trace elements. To explain the temporal evolution of sediment and porewater chemistry, we explore the bacterially mediated oxidation of organic matter as well as alternative biochemical pathways whose relative importance in marine sediments is still a matter of debate.

2 Methodology

2.1 Experimental Design

The experiment was performed in experimental units, composed by sediment and water, enclosed in a glass container (Fig. 1). The sediments were taken in June 2001 from the Capbreton Canyon, in the south-eastern part of the Bay of Biscay, at the site described previously by Anschutz et al. (2002). Multitube-cores were collected and frozen at −25°C. When needed, sediment was defrosted. Around 1 kg of fine sediment with a mean grain size of 9 μm was humidified with 0.45 μm filtered seawater to obtain a mean porosity of 0.80. The sediment slurry was homogenised under oxic conditions. Experimental units were filled by ∼150 ml of this fine sediment, leaving above 12 cm for the gravity deposit and overlying seawater (Fig. 1). The experiment was performed on six experimental units placed in an experimental seawater tank (salinity = 35.5) continuously oxygenated by bubbling air. The experimental tank was kept in the dark at ambient temperature (∼20°C). The fine sediment and water were left to equilibrate for 15 days to form pre-gravity layers (Pre-GL) before adding the gravity layer (GL). Preliminary experiments demonstrated that 15 days were sufficient to obtain well-separated diagenetic zones even if steady-state conditions were reached.

The sediment used to form the GL was composed from fine sand (mean grain size around 150 μm) to mud (mean grain around 9 μm). The sediment was homogenized, and then it was kept under oxic conditions during 10 days prior introducing into the experimental units. About 350 ml of homogenised sediment slurry was rapidly introduced to the overlying water of each experimental unit at day 0 (after the first measurements). Sediment settled slowly during 24 h by gravity and formed the GL, with fine sand at the bottom and mud at the top.

The experiment length was 295 days with five sampling times, which were 1, 7, 33, 75 and 295 days (noted D1, D7, D33, D75 and D295). For each sampling time, one experimental

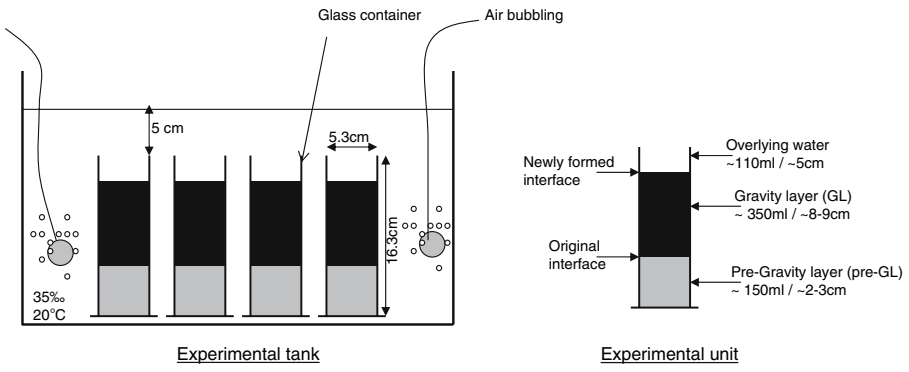

Fig. 1 Experimental system used in the present study. The experimental tank held six experimental units and ∼10 l of filtrated seawater

unit was sacrificed and sub-sampled to separate dissolved (ΣNO_3^-, NO_2^-, NH_4^+, Mn^{2+}, Fe^{2+}) and solid fractions (C_{org}, Mn_{asc}, Fe_{asc}, Mn_{HCl}, Fe_{HCl}). We will detail the analytical methods in Sect. 2.3. Prior to the sub-sampling, vertical profiles of O_2 in sediment porewater were measured using voltammetric microelectrodes. The sixth experimental unit was a reference: O_2, Mn^{2+}, Fe^{2+} and H_2S were monitored by voltammetric microelectrodes prior to D0 (D-1) and at D2, D5, D6, D7, D8, D9, D15, D30, D75 and D295.

2.2 Voltammetric Microelectrode Measurements

Concentrations of O_2, Mn^{2+}, Fe^{2+} and H_2S in the porewaters and in the overlying waters were measured by voltammetry. We used voltammetric gold amalgam microelectrodes made by sealing a 100 μm gold wire in glass tube and plating mercury onto the polished exposed gold surface, as described by Brendel and Luther (1995) and Luther et al. (1998). Measurements were made with an Au/Hg microelectrode as working electrode, a 0.5 mm diameter platinum wire as counter electrode, and a saturated Ag/AgCl electrode as reference electrode. The counter and the references electrodes were introduced at the top of the experimental unit, a few centimetres from the working electrode. An Analytical Instrument Systems, Inc. (AIS) model DLK-100 electrochemical analyser was used for all measurements. Microelectrodes were calibrated for each measurement on the pilot ion method where Mn^{2+} is the standardized ion (Brendel and Luther 1995). Oxygen was determined using Linear Sweep Voltammetry (LSV), scanning from −0.1 to −1.7 V at rate of 200 mV/s without pre-concentration step. Mn^{2+}, Fe^{2+} and H_2S were performed using Cathodic Stripping Voltammetry (CSV) in the square-wave mode, scanning from −0.1 to −1.7 V at rate of 200 mV/s with an equilibration step at −0.1 V for 30 s, scan rate 200 mV/s. Precision for replicates of all species at the same depth is typically below 5%. Detection limits at 99% of confidence limit for O_2, Mn^{2+}, Fe^{2+} and H_2S are 3, 5, 20 and < 0.1 μmol/l, respectively. We used a micromanipulator to obtain millimetre scale depth resolution intervals with minimum sediment disturbance. Microelectrode profiles were made throughout the entirety of experimental units. The vertical resolution steps were 0.5 mm at the newly formed sediment–water interface, 1 mm for the first 10 mm and around the original interface location, and 2–5 mm elsewhere. All profiles were made in different locations in the experimental unit to prevent potential error produced by previous electrode penetration. Analyses were conducted at room temperature ($\sim 20^{\circ}C$).

In this paper, we present mainly O_2 and Mn^{2+} results with some Fe^{2+} results. Since Fe^{2+} signals were complex due to increasing amounts of soluble organic Fe(III) concentration over the experiment, the determination of Fe^{2+} peak height was difficult without specific acquisition methods (Taillefert et al. 2000). The concentrations of H_2S were below the detection limit (<0.1 μmol/l), except on D-1.

2.3 Sample Collection and Treatment

The experimental units were sliced in thin horizontal layers (0.5 cm intervals at the SWI and the original interface and 1 cm below). For each level, a sub-sample was immediately stored in pre-weighed plastic vials and frozen for further analyses of water content and solid phase composition. Another sub-sample was centrifuged under N_2 at 5,000 rpm for 20 min and extracted porewaters were filtered (0.2 μm syringe filter SFCA purged with

N_2). One aliquot was frozen at −25°C for nutrient analysis and another was filtered and acidified to pH 1.6 with trace metal grade HNO_3 for dissolved Fe analysis.

Porosity was determined by comparison of the weight of wet and freeze-dried sediment. Porosity was calculated using a dry sediment density of 2.65 g cm^{-3} (Berner 1980). The freeze-dried solid fraction was homogenised and the water content used to correct the analyses for the presence of sea-salt. Total C concentrations were measured on dry, powdered and homogenized material by infrared spectroscopy using a LECO C-S 125 according to Cauwet et al. (1990). The mean analytical error on total C measurements is ±2%. The inorganic C content of the sediment was determined by coulometric titration of the CO_2 following a 6 N HCl. The precision of inorganic C analyses is estimated at better than ±3%. Organic C (C_{org}) content was then calculated from the difference between total and inorganic C, and thus carries a cumulative uncertainty of about ±5%.

Reactive Fe- and Mn-oxides were determined on homogenised freeze-dried sediments using an ascorbate solution as described by Hyacinthe et al. (2001). Mn and Fe were measured by flame atomic absorption spectrometry (Perkin-Elmer AA 300) using an external aqueous standard for calibration. The reproducibility of the analyses was better than ±3% and ±7% for Mn and Fe, respectively. According to the recent study of Hyacinthe et al. (2006), Fe removed by ascorbate (Fe_{asc}) at near-neutral pH is defined as the reactive pool of reducible Fe(III). Anschutz et al. (2005) showed that the ascorbate reagent was able to extract selectively Mn(III, IV)-oxides (Mn_{asc}) in marine sediment.

Total nitrate ($\Sigma NO_3 = NO_3^- + NO_2^-$) and NO_2^- were analysed by the flow injection described by Anderson (1979). Ammonium (NH_4^+) was analysed by flow-through conductivity method (Hall and Aller 1992). The precision of the N-species analytical procedures was better than 5%. Dissolved Fe concentrations in acidified porewater samples were determined by the ferrozine procedure (Stookey 1970). The precision was better than 10%.

2.4 Flux Calculations

In the absence of re-suspension and bioturbation, molecular diffusion is the main transport mechanism of solute species in muddy sediment (Berner 1980). The vertical diffusive flux of dissolved species is directly proportional to concentration gradient ($\delta C/\delta Z$). In the sediment, it is calculated using Fick's first law as:

$$J = -\phi D_s(\delta C/\delta Z)$$

where J is the flux (nmol/cm^2/d), φ the porosity, and D_s is the bulk sediment diffusion coefficient corrected by tortuosity, i.e. $D_s = D_0/\theta^2$, where θ is tortuosity and D_0 is the molecular diffusion coefficient in water (Berner 1980). The D_0 values obtained from the literature (Schulz 2000) were corrected for in-situ temperature at the time of sampling; tortuosity (θ) was assumed to be equal to $1 - \ln(\varphi^2)$ (Boudreau 1996).

3 Results and Discussion

3.1 Redox Conditions Prior to the Deposition of the Gravity Deposit (D-1)

The thickness of the Pre-GL was ~7 cm. The vertical distributions of O_2, Mn^{2+} and Fe^{2+} in sediment porewaters of individual experimental unit mirror those measured in the sixth

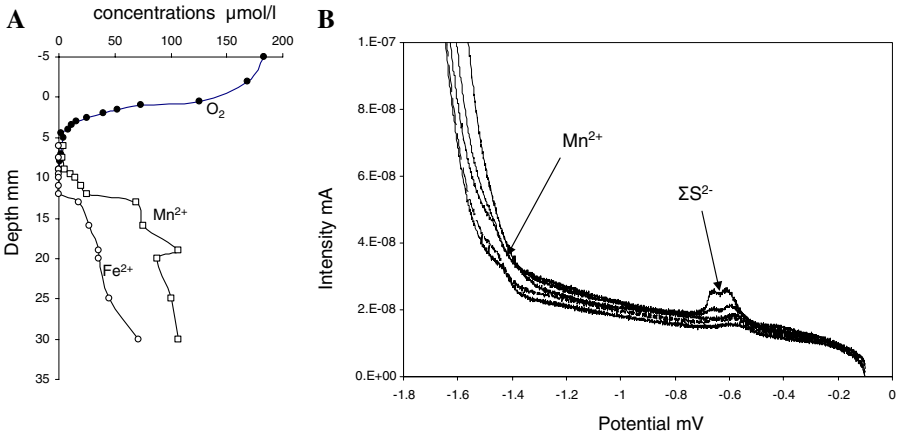

Fig. 2 (**A**) Vertical profiles of O_2, Mn^{2+} and Fe^{2+} (in µmol/l) in the pre-GL of the sixth experimental unit. Measurements were performed prior to the deposition of the GL. Each point represents duplicate microelectrode measurements at the given depth in mm. (**B**) Voltammograms in the square-wave mode. The individual voltammograms were performed independently in the sediment slurry. Peaks located at −1.56 and −0.62 V correspond to Mn^{2+} and ΣH_2S, respectively. The more negative peak at -0.62 V is typical of S(0) in polysulphides (Luther et al. 2001)

reference unit (Fig. 2A). The distributions followed the standard depth sequence of diagenetic reactions (De Lange 1986; Froelich et al. 1979; Postma and Jakobsen 1996) with a thin oxic horizon (∼7 mm) and an anoxic sediment enriched in reduced species (Mn^{2+}, Fe^{2+}).

Voltammetric measurements were carried out at D-1 in the sediment slurry (Fig. 2B). Although the slurry was continuously mixed under oxic conditions, voltammograms exhibited no trace of O_2. However, the scans revealed the presence of Mn^{2+}, H_2S and traces of polysulphides (as shown with the doublet near −0.6 V; Luther et al. 2001).

3.2 Redox Conditions Following the Deposition of the Gravity Layer Over the Experiment

After the introduction of GL, two distinct layers separated by a non-erosive contact were obtained within each experimental unit. Porosity decreased from 0.9 to 0.75, from the top to the bottom (Fig. 3). Minimal values (∼0.5) measured immediately above the original interface reflected the presence of coarse grain particles at the base of the GL.

Organic carbon concentration (C_{org}; Fig. 3) was 2 wt% at the new SWI and decreased to 1.0 wt% in the coarse grain horizon of the GL. The original interface was slightly enriched in C_{org} with content reaching ∼2 wt%. This enrichment persisted over the 295-days of experiment (Fig. 3). In the Capbreton Canyon, the hosted organic matter is mostly refractory due to its terrestrial origin (Grémare et al. 2005). The dominant particle transport in this area is probably by gravity, mass or tubidity flow (Mulder et al. 2001) suggesting that the C_{org} has already been degraded in its original depositional settings. This is supported by the slow ecosystem recovery in the Capbreton Canyon (Anschutz et al. 2002), compared to the rapid formation of biogenic structures after the

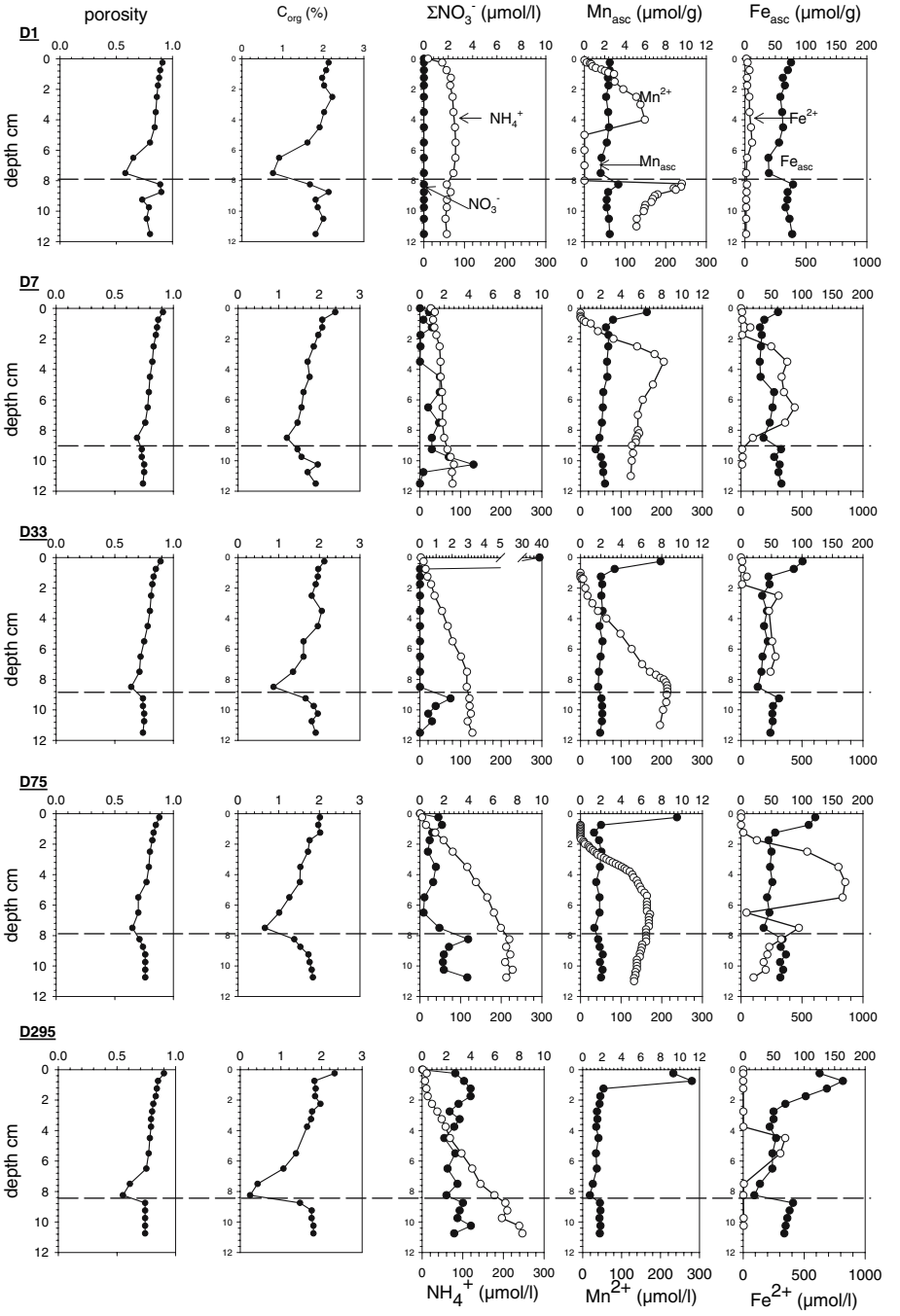

Fig. 3 Time-series profiles of sediment and porewater chemistry measured over the 295-day experiment. The *dashed lines* mark the approximate depth of the original interface. The dissolved Mn^{2+} measured by voltammetric measurements has been added for the appropriate days. The depth is given in centimetre

surge flow event observed in Saguenay fjord (Michaud et al. 2003). The refractory quality of the residual organic matter might limit microbial respiration. A simple mass balance calculations, based on the measured porosity, and C_{org} content (Fig. 3), indicated that only 0.2 wt% of C_{org} within the GL was consumed over the experiment.

3.3 The Temporal Evolution of Dissolved Oxygen

Thirty-five minutes following the deposition, voltammetric techniques did not detect dissolved O_2 at the original interface. The time required to remove all O_2 present initially at the original interface was estimated assuming that the O_2 consumption rate corresponded to the sediment O_2-demand prior to the introduction of the GL. Using the concentration gradient measured between 0 and 1 mm at D-1 (Fig. 2A) and assuming O_2 transport by molecular diffusion, we calculated an O_2-demand of 5.5 mmol/m^2/d for the pre-GL. We concluded that about 50 min were required to completely remove the stock of O_2 present within the original oxic horizon. This time is slightly longer than the time observed in our simulation (<35 min) suggesting another source of O_2 consumption. The high-reduced chemical species pool brought within the sediment slurry above the original interface probably rapidly consumed O_2. This finding supports the suggestion that anoxic conditions rapidly settled following mass flow deposits.

Anoxic conditions prevailed within the slurry (Fig. 2B), and O_2 was totally absent during the gravity settling. After a few hours, an oxic layer formed at the new sediment–water interface. Oxygen diffused from the oxygenated overlying water to the first millimetre of sediment (D2, Fig. 4). The shape of the O_2 profile measured at D2 indicated that O_2 was directly consumed in the overlying water. Oxygen is the first oxidant to be used by microbial oxidation of organic matter. In addition, here, O_2 was consumed to oxidize reduced compounds, such as NH_4^+, Mn^{2+}, Fe^{2+} and H_2S, that escaped from the new material. Using the concentration gradients between 0 and 1 mm depth at D2 (Fig. 4), we estimated a downward O_2 flux of 6.0 mmol/m^2/d. The oxic layer extended to 5 mm depth on the fifth day (D5) and then, it persisted at this depth. The sediment O_2-demand ranged between 8.93 and 5.67 mmol/m^2/d (mean values 7.23 ± 1.15 mmol O_2/m^2/d, n = 10) over the experiment.

3.4 The Temporal Evolution of Manganese

The temporal evolution of dissolved Mn concentrations measured by voltammetric microelectrodes is reported in Fig. 5. Troubles with electrode calibration prevented Mn^{2+} concentration measurements at D295. Traces of dissolved Mn were already detected within the slurry (Fig. 2B). During the experiment, Mn^{2+} concentrations fluctuated between 0 and 300 µmol/l.

Manganese concentrations increased with depth within the GL. The pool of Mn^{2+} in porewaters is replenished by the progressive reductive dissolution of Mn-oxides brought within GL. Dissolved Mn diffused both upward to the new sediment–water interface, and downward to the base of the GL and to the Pre-GL. Oxygen is an efficient oxidant for Mn^{2+}. The oxidation kinetics of Mn^{2+} by O_2 is slow in artificial water (Diem and Stumm 1984; Stumm and Morgan 1996). It becomes orders of magnitude faster in the presence of Mn-bacteria and surface catalysts (Sung and Morgan 1981). In addition, disturbances and oscillatory conditions stimulate microbial reaction rates in natural sediments (Aller and

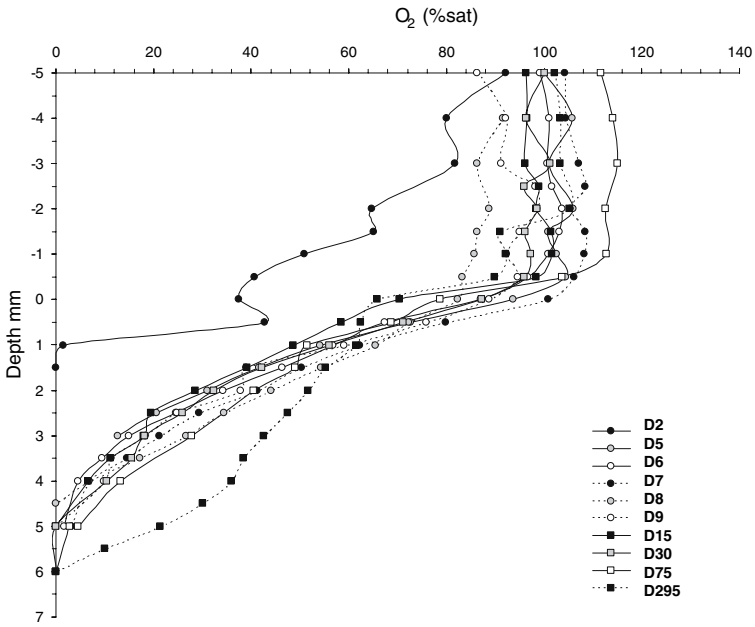

Fig. 4 Time-series profiles of dissolved O_2 (in % of saturation) measured using LSV microelectrodes. Each point represents duplicate microelectrode measurements at the given depth (mm)

Aller 1998). The continuous diffusion of O_2 rapidly promoted the precipitation of fresh authigenic Mn(III, IV)-oxides at the new established oxic horizon, as observed in Fig. 3 (Mn_{asc}). The depth at which dissolved Mn was detected first, however, moved down to 15 mm from D15 to D75 (Fig. 5). A detailed examination revealed that the Mn^{2+} profiles did not overlap the profile of O_2, except for the first days of the experiment. This suggests either that O_2 was not the only candidate for the oxidation of Mn^{2+} in sediment, or that adsorption (no oxidation) was the process of Mn^{2+} removal. Iodate (IO_3^-) is capable to oxidize Mn^{2+} (Anschutz et al. 2000). However, iodide (I^-), which is the reduced form of iodate, was not detected by the voltammetric technique (detection limit <0.2 µmol/l). The continuous precipitation of Fe(III)- and Mn(III, IV)-oxides favoured Mn^{2+} adsorption (Burdige et al. 1992; Stiers and Schwertmann 1985; van der Zee et al. 2001) and could limit the diffusion of Mn^{2+} to the newly established oxic horizon.

During the first days of the experiment (D2 to D15), Mn^{2+} concentrations decreased towards the original interface, suggesting a sink of Mn in the anoxic Pre-GL. In anoxic conditions, sorption of Mn^{2+} onto $CaCO_3$ surfaces is the most important processes that control the mobility of Mn^{2+} (Middelburg et al. 1987; Mucci 2004). The rapid O_2 depletion, and the subsequent reduction of Fe–Mn-oxides that followed the gravity settling might produce sufficient alkalinity to favour the precipitation of carbonate. As porewaters become supersaturated with respect to calcite and rhodochrosite, Mn^{2+} is most likely precipitated as a mixed carbonate phase. The affinity of Mn^{2+} for Fe-monosulphides has been recognized (Arakaki and Morse 1993), and AVS brought within the sediment slurry might act as an efficient sink for dissolved Mn as well.

Beginning the first day, high Mn^{2+} concentrations were measured at the original interface. The concomitant presence of high Mn^{2+} concentrations and Mn(III/IV)-oxides

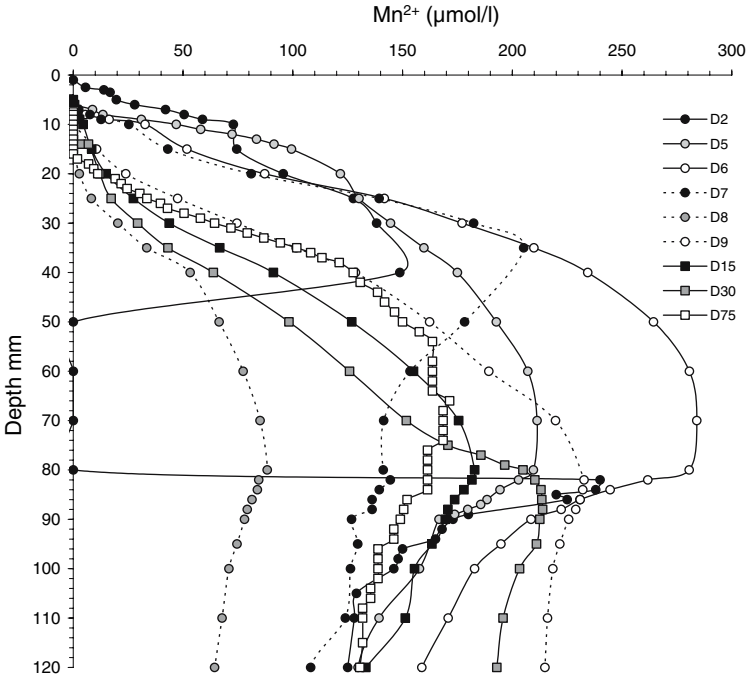

Fig. 5 Time-series profiles of dissolved Mn^{2+} (in µmol/l) measured using CSV microelectrodes. Each point represents duplicate microelectrode measurements at the given depth (mm). Details on the upward flux calculations are given in Table 1

(D1; Fig. 3) that were relict from the original oxic horizon, clearly indicates that Mn-oxides were reduced during the experiment. Mn_{asc}-profiles (Fig. 3) are in agreement with the reductive dissolution of Mn-oxides at the original interface. The inventory of Mn_{asc} within each experimental unit was around 372 ± 40 µmol, with ~70% contained within the GL. These amounts remained constant throughout the experiment, indicating that the Pre-GL was not a significant source of Mn to the GL. Within the GL, the progressive surficial enrichment corresponded to a Mn_{asc} accumulation of 17.0, 42.3, 64.6 and 72.6 µmol at D7, D33, D75 and D295, respectively. Using voltammetric profiles (Fig. 5), upward diffusive fluxes of dissolved Mn were estimated. Table 1 shows the details of flux calculations. The time integration of these fluxes permitted to estimate the accumulated Mn_{asc} by diffusion. These calculations are consistent with the Mn_{asc} inventory, confirming that a steady-state model permits to describe the recycling of Mn-oxide compounds in turbidites (Anschutz et al. 2002).

3.5 The Temporal Evolution of Iron

The time-series profiles of reactive Fe(III)-oxides (Fe_{asc}, Fig. 3) were characterized by the development of a surficial peak at the new SWI. Released Fe from anoxic sediments was progressively oxidized and precipitated at the top of the GL. The first day, Fe^{2+} was detected directly in the overlying water, indicating that Fe escaped from the new material

Table 1 Parameters used to assess the cumulative Mn excess at the new sediment–water interface

Days	Interval depth (mm)	Mn^{2+} gradients (μmol/cm)	Mn^{2+} upward fluxes (mmol/m^2/d)	Cumulative Mn content (μmol)
2	2.5–10.0	56.16	0.19	2.74
5	7.0–10.0	127.23	0.79	16.60
6	7.0–10.0	136.25	0.47	33.23
7	7.0–10.0	75.96	0.26	44.05
8	10.0–20.0	23.20	0.08	45.18
9	15.0–25.0	17.56	0.13	47.20
15	15.0–25.0	22.04	0.07	48.94
30	15.0–25.0	17.24	0.36	50.84
75	15.0–25.0	53.18	0.16	71.51

The first Fick's law has been applied using a diffusive coefficient $D_0(Mn^{2+}$ at 20°C) = 5.44×10^{-6} cm^2/s

(11.7 μmol/l in the overlying water; Fig. 3). However, Fe^{2+} concentrations remained low (<50 μmol/l) within the whole experimental unit. The preferential use of Mn-oxides as electron acceptors by microbial respiration could have hindered the microbial reduction of Fe-oxides. Oxygen was probably the main oxidant for escaped Fe^{2+}. The downward flux of O_2 (i.e. 6.0 mmol/m^2/d) was large enough to oxidize the upward flux of Fe^{2+} (0.13 mmol/m^2/d; Table 2). After a few days, dissolved Fe^{2+} was detected first below the surficial Mn(III/IV)-oxides rich horizon (Fig. 3). Oxidation of Fe^{2+} occurs under both aerobic and anaerobic conditions. It can be microbially mediated and non-enzymatic. At circumneutral pH, non-enzymatic anaerobic oxidation reactions are rapid (Straub et al. 2001). Manganese (III/IV)-oxide is an efficient oxidant for Fe^{2+} (Hyacinthe et al. 2001; Myers and Nealson 1988; Postma 1985). The Mn rich horizon acted as an oxidative barrier that limited the diffusive loss of Fe from sediment. This anaerobic oxidation pathway formed a pool of fresh Fe(III)-oxides usable by dissimilatory Fe(III)-reducing bacteria. Trace amounts of NO_3^- could also act as oxidant for Fe^{2+}. The reduction of NO_3^- to N_2 by Fe^{2+} is thermodynamically favourable at all pH encountered in marine sediments (Luther et al. 1997). The upward fluxes of Fe^{2+} varied from 0.28 and 0.63 mmol/m^2/d over the experiment. According to the stoichiometry of the reaction (one NO_3^- can oxidize five Fe^{2+}), the

Table 2 Vertical fluxes of dissolved species in mmol/m^2/d (negative and positive values correspond to downward and upward fluxes, respectively) calculated from dissolved gradients

Days	O_2^a	Mn^{2+b}	Fe^{2+c}	NO_3^{-d}	NH_4^{+e}
1	−6.00	0.19	0.13	–	7.1×10^{-2}
7	−8.50	0.26	0.44	–	0.8×10^{-2}
33	−6.90	0.04	0.28	-5.2×10^{-2}	1.3×10^{-2}
75	−5.90	0.16	0.63	-0.2×10^{-2}	3.7×10^{-2}
295	−7.00	–	–	-0.2×10^{-2}	2.3×10^{-2}

[a] $D_0(O_2$ at 20°C) = 1.91×10^{-5} cm^2/s

[b] $D_0(Mn^{2+}$ at 20°C) = 5.44×10^{-6} cm^2/s

[c] $D_0(Fe^{2+}$ at 20°C) = 5.91×10^{-6} cm^2/s

[d] $D_0(NO_3^-$ at 20°C) = 1.62×10^{-6} cm^2/s

[e] $D_0(NH_4^+$ at 20°C) = 1.66×10^{-6} cm^2/s

downward fluxes of NO_3^- (i.e. 0.052–0.002 mmol/m^2/d) were unable to oxidize all Fe^{2+} in the experimental units. Note that soluble organic Fe(III) have been progressively detected over the experiment by voltammetric analyses (data not shown). The exact mechanisms by which soluble Fe(III) forms and persists is still a matter of debate, but its occurrence in marine sediments might accelerate the microbial-mediated oxidation of organic matter as well as other biochemical pathways involving Fe.

The stocks of surficial Fe(III)-oxides were equal to 1.0, 0.8, 1.3, 1.6 and 2.5 mmol at D1, D7, D33, D75 and D295, respectively. At the end of the experiment, this stock represented an accumulation superior to 20% of the reactive Fe-oxides inventory. In marine sediments, reduced Fe precipitates as a variety of Fe-minerals. The time integration of upward Fe^{2+} fluxes (Table 2) permits an estimate of the amount of Fe that diffused to the top of the GL. The estimations are equal to 0.3, 7.5, 29 and 195 µmol of Fe. These results are inferior to the inventory of surficial accumulated Fe_{asc}. A great part of the surficial accumulated Fe(III)-oxides (>70%) probably originated from the oxidation (without mobilization in porewater) of reduced Fe(II)-bearing phases (i.e. mostly as FeS and FeS_2) that were initially present at the top of the GL. We conclude that a steady-state model based only on the oxidation of dissolved reduced Fe(II) cannot describe the cycling of Fe-oxides probably because of multiple Fe sources.

At the original interface, Fe_{asc} remained mostly immobile (Fig. 3). A mass balance calculation confirmed that the Fe_{asc} content remained almost constant ($\sim$40% of the Fe_{asc} inventory) within the Pre-GL. Reduced Fe released from the microbial reduction of reactive Fe(III)-oxide reacts with authigenic Mn(III/IV)-oxides or NO_3^-. These anaerobic oxidation pathways might replenish the Fe(III)-oxides pool at the original interface as long as oxidants are present.

3.6 The Temporal Evolution of Nitrogen Species

At D1, NO_3^- and NO_2^- were below the detection limit throughout the whole experimental unit (Fig. 3, Table 3). NH_4^+ was detected in both the sediment and the overlying water. Initial anaerobic conditions within the slurry prevented the NO_2^-/NO_3^- production by microbial nitrification because nitrification occurs under strictly aerobic conditions (or microaerobic zones). At the original interface, the microbial consumption of ΣNO_3 (NO_2^- + NO_3^-) by respiratory denitrification was probably simultaneous to the deposition. Nitrate reduction can also be supported by electron donors other than organic matter such as Fe^{2+} and Mn^{2+} (Sørensen and Jørgensen 1987; Postma 1990; Aller 1994; Luther et al. 1997, 1998). Reduction of NO_3^- by sulphides species (H_2S, S^0, HS^-) are also thermodynamically favourable (Jørgensen and Nelson 2004). These mechanisms proceed via a complex web of reactions controlled by both biotic and abiotic processes.

The time-series profiles of ΣNO_3 were characterized by a progressive enrichment located at both the new SWI and the original interfaces. At the new SWI, the downward fluxes of O_2 were large enough to oxidize the upward fluxes of NH_4^+ to produce NO_3^- (Table 2). Nitrification should be coupled to simultaneous denitrification. Direct oxidation of NH_4^+ by either NO_3^- (Mulder et al. 1995) or NO_2^- (van de Graaf et al. 1995) to N_2 occurs under anaerobic conditions. The simultaneous presence of NH_4^+ and NO_2^- under oxygen-depleted conditions is a prerequisite for Anammox (ANoxic AMMonium OXidation). This reaction competes with the oxidation of NH_4^+ to NO_3^- at the oxic horizon. Unfortunately, the relative contribution of these reactions could not be established in our experiment.

Table 3 Down-core concentrations of N-species in µmol/l

D1				D7				D33				D75				D295			
Depth (cm)	ΣNO_3 (µmol/l)	NO_2^- (µmol/l)	NH_4^+ (µmol/l)	Depth (cm)	ΣNO_3 (µmol/l)	NO_2^- (µmol/l)	NH_4^+ (µmol/l)	Depth (cm)	ΣNO_3 (µmol/l)	NO_2^- (µmol/l)	NH_4^+ (µmol/l)	Depth (cm)	ΣNO_3 (µmol/l)	NO_2^- (µmol/l)	NH_4^+ (µmol/l)	Depth (cm)	ΣNO_3 (µmol/l)	NO_2^- (µmol/l)	NH_4^+ (µmol/l)
0.00	<dl	<dl	10.00	0.00	<dl	<dl	26.35	0.00	38.79	28.44	2.13	0.00	<dl	<dl	0.29	0.00	<dl	<dl	1.39
0.25	<dl	<dl	44.85	0.25	0.74	<dl	36.26	0.25	27.48	–	8.78	0.25	1.51	0.16	5.17	0.25	2.72	0.15	11.13
0.75	<dl	<dl	55.60	0.75	0.27	<dl	31.97	0.75	<dl	–	13.78	0.75	1.80	0.37	14.65	0.75	3.44	0.23	6.96
1.25	<dl	<dl	66.38	1.25	0.97	–	35.19	1.25	<dl	<dl	18.06	1.25	1.01	0.31	37.34	1.25	3.98	1.02	10.20
1.75	<dl	<dl	64.76	1.75	<dl	–	40.02	1.75	<dl	–	27.15	1.75	0.79	–	58.02	1.75	3.98	0.94	13.45
2.50	<dl	<dl	70.70	2.50	<dl	<dl	48.07	2.50	<dl	–	35.73	2.50	0.65	–	80.72	2.25	2.99	0.35	24.12
3.50	<dl	<dl	72.86	3.50	<dl	–	50.22	3.50	<dl	–	53.99	3.50	1.30	–	116.34	2.75	2.26	<dl	37.10
4.50	<dl	<dl	76.64	4.50	1.63	1.63	50.76	4.50	<dl	<dl	68.00	4.50	1.08	–	137.88	3.25	3.08	–	47.77
5.50	<dl	<dl	78.26	5.50	1.62	1.62	53.99	5.50	<dl	–	80.42	5.50	0.36	–	165.74	3.75	2.63	–	57.51
6.50	<dl	<dl	77.72	6.50	0.67	0.67	55.60	6.50	<dl	<dl	101.01	6.50	0.29	–	182.12	4.50	1.81	–	68.64
7.50	<dl	<dl	72.86	7.50	1.56	1.56	55.07	7.50	<dl	<dl	115.69	7.50	1.59	–	199.35	5.50	2.72	1.81	96.93
8.25	<dl	<dl	56.14	8.50	0.97	0.59	59.37	8.50	<dl	–	115.15	8.25	3.96	–	220.03	6.50	2.78	2.77	123.36
8.75	<dl	<dl	65.84	9.25	0.97	<dl	67.46	9.25	1.90	–	121.68	8.75	2.38	–	211.99	7.50	2.90	2.80	143.30
9.25	<dl	<dl	56.68	9.75	2.36	–	75.56	9.75	0.97	–	122.23	9.25	4.23	3.52	222.33	8.25	1.99	–	178.09
9.75	<dl	<dl	56.14	10.25	4.40	–	83.67	10.25	0.51	–	125.50	9.75	1.87	1.26	209.69	8.75	3.35	–	204.99
10.50	<dl	<dl	52.91	10.75	0.27	<dl	78.80	10.75	0.74	–	117.33	10.25	1.95	1.20	228.08	9.25	3.08	–	209.62
11.50	<dl	<dl	56.14	11.50	<dl	<dl	80.42	11.50	<dl	–	129.32	10.75	3.89	1.11	212.57	9.75	2.90	–	196.17

dl: limit of detection = 0.1 µmol/l

–: no data (the volume of porewater was to low)

Nitrate concentrations increased with time in the anoxic part of the Pre-GL as well as in the GL (Fig. 3). Concentrations reached values close to 4 μmol/l at the previous interface. In the absence of any evidence of water infiltration, the occurrence of ΣNO_3 within the overall experimental units suggests an anoxic ΣNO_3 production as observed in the post-flood deposit in the Saguenay Fjord (Deflandre et al. 2002) and in the Capbreton Canyon (Anschutz et al. 2002). Field and experimental studies indicated that anaerobic oxidation of NH_4^+ to NO_3^- could be supported by Mn(III/IV)-oxides (Anschutz et al. 2005; Hulth et al. 1999; Luther and Popp 2002; Mortimer et al. 2004). Anschutz et al. (2005) estimated that the oxidation of NH_4^+ by Mn(III/IV)-oxides was energetically possible under typical sedimentary conditions. Probably because of the multiple pathways to reduce ΣNO_3 to N_2 under anoxic conditions (e.g. potential oxidants: C_{org}, Fe^{2+}, NH_4^+, H_2S, AVS), the concentration of ΣNO_3 remained weak (<5 μmol/l). In addition, the occurrence of NO_2^- at the same locations is in agreement with denitrifying processes (Table 3).

4 Summary and Conclusion

This experimental study presents for the first time the succession of diagenetic reactions that follow the deposition of GL a few cm-thick. The use of voltammetric microelectrodes was an appropriate technique to gain information into the natural dynamics of oxygen and dissolved Mn in disturbed sediments. The temporal evolution of Mn species indicated that a steady-state model allows us to describe the recycling of Mn in turbidites. In contrast, profiles of NO_3^-, NH_4^+ and Fe never reached steady state over the experimental period, probably because of their complex sources, sinks and reactivity in the sediment. In this experiment, the complete benthic ecosystem recovery required more than 10 months clearly demonstrating that surge flow events deeply affected the ongoing diagenesis of underlying sediments, even if a new material layer covers only a few centimetres thickness. A complex web of reactions governs the diagenetic processes during the sedimentary recovery and alternative metabolic pathways might dominate heterotrophic dissimilatory reactions. Many of these reactions and pathways need further investigations under natural environmental conditions. However, their reproduction in experimental studies confirms their relative importance under natural non-steady conditions.

Acknowledgements We thank the assistance of the crew of the "Côte de la Manche" and the participants of the Sedican cruises for help in the field. This research was funded by the program PROOF of the Institut National des Sciences de l'Univers - CNRS. We thank also the editorial reviewers whose comments inspired us to improve our manuscript. Gwenaëlle Chaillou expresses her special gratitude to Pr. G. W. Luther III, who worked hard to review the manuscript. This is a contribution of the UMR 5805 EPOC.

References

Aller JY (1989) Quantifying sediment disturbance by bottom currents and its effects on benthic communities in a deep-sea western boundary zone. Deep Sea Res Part A Oceanogr Res Papers 36:901–934

Aller RC (1994) The sedimentary Mn cycle in Long Island Sound: its role as intermediate oxidant and the influence of bioturbation, O_2, and C_{org} flux on diagenetic reaction balances. J Marine Res 52:259–295

Aller RC, Aller JY (1998) The effect of biogenic irrigation intensity and solute exchange on diagenetic reaction rates in marine sediments. J Marine Res 56:905–936

Anderson L (1979) Simultaneous spectrophotometric determination of nitrite and nitrate by flow injection analysis. Anal Chim Acta 110:123–128

Anschutz P, Dedieu K, Desmazes F, Chaillou G (2005) Speciation, oxidation state, and reactivity of particulate manganese in marine sediments. Chem Geol 218:265–279

Anschutz P, Sundby B, Lefrançois L, Luther GWI, Mucci A (2000) Interaction between metal oxides and nitrogen and iodine in bioturbated marine sediments. Geochim Cosmochim Acta 64:2751–2763
Anschutz P, Jorissen FJ, Chaillou G, Abu-Zied R, Fontanier C (2002) Recent turbidite deposition in the eastern Atlantic: early diagenesis and biotic recovery. J Marine Res 60:835–854
Arakaki T, Morse JW (1993) Coprecipitation and adsorption of Mn(II) with machinawite (FeS) under conditions similar to those found in anoxic sediments. Geochim Cosmochim Acta 57:9–14
Berner RA (1980) Early diagenesis: theoretical approach. Princeton University Press, Princeton, NJ
Boudreau BP (1996) The diffusive tortuosity of fine-grained unlithified sediments. Geochim Cosmochim Acta 60:3139–3142
Brendel PJ, Luther GWI (1995) Development of a gold amalgam voltammetric microelectrode for the determination of dissolved Fe, Mn, O_2, and S(-II) in porewaters of marine and fresh-water sediments. Environ Sci Technol 29:751–761
Buckley DE, Cranston RE (1988) Early diagenesis in deep-sea turbidites—the imprint of paleo-oxidation zones. Geochim Cosmochim Acta 52:2925–2939
Burdige DJ, Dhakar SP, Nealson KH (1992) Effects of manganese oxide mineralogy on microbial and chemical manganese reduction. Geomicrobiol J 10:27–48
Cauwet G, Gadel F, de Souza Sierra MM, Donard OFX, Ewald M (1990) Contribution of the Rhône River to organic carbon inputs to the Northwestern Mediterranean Sea. Continental Shelf Res 10:1025–1037
Colley S, Thomson J (1985) Recurrent uranium relocations in distal turbidites emplaced in pelagic conditions. Geochim Cosmochim Acta 49:2339–2348
De Lange GJ (1986) Early diagenetic reaction in interbeded pelagic and turbiditic sediments in the Nares Abyssal Plain (Western North Atlantic): consequences for the composition of sediment and interstitial water. Geochim Cosmochim Acta 50:2543–2561
Deflandre B, Mucci A, Gagné J-P., Guignard C, Sundby B (2002) Early diagenetic processes in coastal marine sediments disturbed by a catastrophic sedimentation event. Geochim Cosmochim Acta 66:2547–2558
Diem D, Stumm W (1984) Is Mn^{2+} being dissolved by O_2 in absence of Mn-bacteria of surfaces catalysts? Geochim Cosmochim Acta 48:1571–1573
Froelich PN, Klinkhammer GP, Bender ML, Luedke NA, Heath GR, Cullen D, Dauphin P, Hammond D, Hartman B, Maynard V (1979) Early oxidation of organic matter in pelagic sediments of the Eastern Equatorial Atlantic: suboxic diagenesis. Geochim Cosmochim Acta 43:1075–1090
Grémare A, Guttierez D, Anschutz P, Deflandre B, Vétion G, Zudaire L (2005) Spatio-temporal changes in totally and enzymatically hydrolisable amino acids of superficial sediments from three contrasted areas. Prog Oceanogr 65:89–111
Hall POJ, Aller RC (1992) Rapid, small-volume flow injection analysis for CO_2 and NH_4^+ in marine and freshwaters. Limnol Oceanogr 37:1113–1119
Hulth S, Aller RC, Gibert F (1999) Coupled anoxic nitrification/manganese reduction in marine sediments. Geochim Cosmochim Acta 63:49–66
Hyacinthe C, Bonneville S, Van Cappellen P (2006) Reactive iron(III) in sediments: chemical versus microbial extractions. Geochim Cosmochim Acta 70:4166–4180
Hyacinthe C, Anschutz P, Jouanneau J-M, Jorissen FJ (2001) Early diagenesis processes in the muddy sediment of the Bay of Biscay. Marine Geol 177:111–128
Jarvis I, Pearce T, Higgs N (1988) Early diagenetic geochemical trends in quaternary distal turbidites. Chem Geol 70:10–10
Jørgensen BB, Nelson DC (2004) Sulphide oxidation in marine sediment: geochemistry meets microbiology. In: Geological Society of America (ed) Sulphur biogeochemistry—past and present, Special papers 379, pp 63–81
Luther GW III, Sundby B, Lewis BL, Brendel PJ, Silverberg N (1997) Interactions of manganese with nitrogen cycle: alternative pathways to dinitrogen. Geochim Cosmochim Acta 61:4043–4052
Luther GW III, Brendel PJ, Lewis BL, Sundby B, Lefrancois L, Silverberg N, Nuzzio D (1998) Oxygen, manganese, iron, iodide, and sulfide distributions in pore waters of marine sediments measured simultaneously with a solid state voltammetric microelectrode. Limnol Oceanogr 43:325–333
Luther GW III, BT Glazer, Hohman L, Popp JI, Taillefert MT, Rozan F., Brendel PJ, Theberge SM, Nuzzio DB (2001) Sulfur speciation monitored in situ with solid state gold amalgam voltammetric microelectrodes: polysulfides as a special case in sediments, microbial mats and hydrothermal vent waters. J Environ Monit 3:61–66
Luther GW III, Popp JI (2002) Kinetics of the abiotic reduction of polymeric manganese dioxide by nitrite: an anaerobic nitrification reaction. Aquat Geochem 8:15–36
Megonigal JP, Hines ME, Visscher PT (2004) Anaerobic metabolism: linkage to trace gases and anaerobic processes. In: Schlesinger WH (ed) Biogeochemistry 8. Elsevier-Pergamon, Oxford, UK

Michaud E, Desrosiers G, Long B, de Montety L, Crémer J-F, Pelletier E, Locat J, Gilbert F, Stora G (2003) Use of axial tomography to follow temporal changes of benthic communities in an unstable sedimentary environment (Baie des Ha! Ha! Saguenay Fjord). J Exp Marine Biol Ecol 285–286:265–282

Middelburg JJ, De Lange GJ, Van Der Weijden CH (1987) Manganese solubility in marine porewaters. Geochim Cosmochim Acta 51:759–763

Mortimer RJG, Harris SJ, Krom MD, Freitag T, Prosser J, Barnes J, Anschutz P, Hayes P, Davies IM (2004) Anoxic nitrification in marine sediments. Marine Ecol Prog Ser 276:37–51

Mucci A (2004) The behaviour of mixed Ca-Mn carbonates in water and seawater: controls of manganese concentrations in marine porewaters. Aquat Geochem 10:139–169

Mucci A, Edenborn HM (1992) Influence of an organic-poor landslide deposit on the early diagenesis of iron and manganese in a coastal marine sediment. Geochim Cosmochim Acta 56:3909–3921

Mucci A, Boudreau B, Guignard C (2003) Diagenetic mobility of trace elements in sediments covered by a flash flood deposit: Mn, Fe, and As. Appl Geochem 18:1011–1026

Mulder A, van de Graaf AA, Robertson LA, Kuenen JG (1995) Anaerobic ammonium oxidation discovered in denitrifying fluidized bed reactor. FEMS Microbiol Ecol 16:177–184

Mulder T, Weber O, Anschutz A, Jorissen FJ, Jouanneau JM (2001) A few months-old storm-generated turbidite deposited in the Capbreton Canyon (Bay of Biscay, SW France). Geo-Marine Lett 21: 149–156

Myers CR, Nealson KH (1988) Microbial reduction of manganese oxides: interactions with iron and sulfur. Geochim Cosmochim Acta 54:2727–2732

Postma D (1985) Concentration of Mn and separation from Fe in sediments. I. Kinetics and stoichiometry of the reaction between birnessite and dissolved Fe(II) at 10 8C. Geochim Cosmochim Acta 49:1023–1033

Postma D (1990) Kinetics of nitrate reduction by detrital Fe(II)-silicates. Geochim Cosmochim Acta 54:903–908

Postma D, Jakobsen R (1996) Redox zonation: equilibrium constrains on the Fe(III)/SO_4-reduction interface. Geochim Cosmochim Acta 60:3169–3175

Saulnier I, Mucci A (2000) Trace metal remobilization following the resuspension of estuarine sediments: Saguenay Fjord, Canada. Appl Geochem 15:191–210

Schulz H (2000) Quantification of early diagenesis: dissolved constituents in marine pore water. In: Schulz HD, Zabel M (eds) Marine geochemistry. Springer, Berlin

Sørensen J, Jørgensen BB (1987) Early diagenesis in sediments from Danish coastal waters: Microbial activity and Mn–Fe–S geochemistry. Geochim Cosmochim Acta 51:1583–1590

Stiers W, Schwertmann U (1985) Evidence for manganese substitution in synthetic goethite. Geochim Cosmochim Acta 49:1909–191

Stookey LL (1970) Ferrozine—a new spectrophotometric reagent for iron. Anal Chem 42:779–781

Straub KL, Benz M, Schink B (2001) Iron metabolism in anoxic environments at near neutral pH. FEMS Microbiol Ecol 34:181–186

Stumm W, Morgan JJ (1996) Aquatic chemistry: chemical equilibria and rates in natural waters, 3rd edn. Wiley, New York

Sundby B (2006) Transient state diagenesis in continental margin mud. Marine Chem 102:2–12

Sung W, Morgan JJ (1981) Oxidative removal of Mn^{2+} from solution catalysed by the g-FeOOH (lepidocrosite) surface. Geochim Cosmochim Acta 45:2377–2383

Taillefert M, Bono AB, Luther GW III (2000) Reactivity of freshly formed Fe(III) in synthetic solutions and (pore)waters: voltammetric evidence of an aging process. Environ Sci Technol 34:2169–2177

van de Graaf AA, Mulder A, de Bruijn P, Jetten MSM, Robertson LA, Kuenen JG (1995) Anaerobic oxidation of ammonium is a biologically mediated process. Appl Environ Microbiol 61:1246–1251

van der Zee C, van Raaphorst W, Epping E (2001) Adsorbed Mn^{2+} and Mn redox cycling in Iberian continental margin sediments (northeast Atlantic Ocean). J Marine Res 59:133–166